Jestr Journal of Engineering Science and Technology Review 8 (5) (2015) 34-40

JOURNAL OF Engineering Science and Technology Review

Research Article

www.jestr.org

Parameter Deduction and Accuracy Analysis of Track Beam Curves in Straddle-type Monorail Systems

Xiaobo Zhao[1,2], Guilin Wang[1,3*], Xianfeng Wu[4] and Jie Zhou[5]

[1]*School of Civil Engineering, Chongqing University, Shaping Road 174#, Shapingba, 400044,Chongqing, China*
[2]*Chongqing Rail Transit Design and Research Institute, Light-Rail Tongjiayuanzi Base, Jintong Road, New North Zone, 401122,Chongqing, China*
[3]*Key Laboratory of New Technology for Construction of Cities in Mountain Area(Chongqing University), Ministry of Education, Chongqing 400045, China;*
[4]*Sino-coal International Engineering Group Chongqing Design & Research Institute, Daping Road 328#, Yuzhong, 400016, Chongqing, China*
[5]*Department of Civil Engineering, Faculty of Engineering, University of Bristol, Queen's Building, University Walk, BS84UD, Bristol, United Kingdom*

Received 10 October 2015; Accepted 21 December 2015

Abstract

The accuracy of the bottom curve of a PC track beam is strongly related to the production quality of the entire beam. Many factors may affect the parameters of the bottom curve, such as the superelevation of the curve and the deformation of a PC track beam. At present, no effective method has been developed to determine the bottom curve of a PC track beam; therefore, a new technique is presented in this paper to deduce the parameters of such a curve and to control the accuracy of the computation results. First, the domain of the bottom curve of a PC track beam is assumed to be a spindle plane. Then, the corresponding supposed top curve domain is determined based on a geometrical relationship that is the opposite of that identified by the conventional method. Second, several optimal points are selected from the supposed top curve domain according to the dichotomy algorithm; the supposed top curve is thus generated by connecting these points. Finally, one rigorous criterion is established in the fractal dimension to assess the accuracy of the assumed top curve deduced in the previous step. If this supposed curve coincides completely with the known top curve, then the assumed bottom curve corresponding to the assumed top curve is considered to be the real bottom curve. This technique of determining the bottom curve of a PC track beam is thus proven to be efficient and accurate.

Keywords: straddle-type monorail, PC track beam curve, dichotomy algorithm, least square method, fractal, accuracy criterion.

1. Introduction

The track beam of a monorail system is generated in three types: precast concrete (PC), reinforced concrete, and steel track beams. The PC track beam is the most commonly used among these types [1],[2]. At present, the bridge system of the monorail track beam can be divided into simply supported and continuous structure systems. The typical spans of a PC track beam in a simply supported structure system are 22and 24 m; this combination is often applied in Chongqing, China and in Japan (Fig. 1). The span of the track beam in a continuous structure system is 30 m; this beam is commonly constructed in Dubai, Malaysia, and Brazil, among others (Fig. 2).

The PC track beam is important in the monorail bridge system because such beams not only comprise the track that guides monorail vehicles but also bears the corresponding loads, including that of the track's own weight (Fig. 3). To ensure the operation safety and comfort of a monorail train, a PC track beam must be adequately sized [3]. This size mainly depends on the bottom curve of this beam during construction [4,5]; nonetheless, only the top beam curve is known at this stage. Although deducing the bottom curve of a PC track beam is significant, no effective method has been developed to determine this curve and to assess the accuracy of computation results. For instance, Xu G [6] determined the bottom curve of a PC track beam based on a given top curve. Zhu Y L [7] identified the manufacturing parameters of a PC track beam through construction control; this approach partly enhances the quantity of PC track beams, although it is time consuming. The conventional technique can approximate the bottom curve of a PC track beam; however, the obtained curve may be inaccurate in complex cases, such as the transition curve, curve superelevation, and vertical curve. Therefore, the current study develops a new method to determine the curves of a PC track beam. The research results generated are of theoretical and practical significance.

The new method not only deduces the curve of a PC track beam based on a geometrical relationship that reverses the one identified by the conventional method but also establishes an effective criterion to assess the accuracy of the obtained curve. First, the method assumes that the domain of the bottom curve of a PC track beam is a spatial spindle plane that is divided into $m \times m$ subsections; this assumption

* E-mail address: glwcqu@qq.com
ISSN: 1791-2377

explains the corresponding $m \times m$ crossover points in the plane. Second, the corresponding $m \times m$ points, which are composed of the domain plane of the assumed top curves, can be easily obtained based on the $m \times m$ points in the assumed bottom curve plane; these points can be determined according to the geometrical relationship that is the opposite of that identified by the conventional method. Third, the point that is nearest to the known top curve in any row of the assumed top curve plane can be quickly derived with the dichotomy algorithm. This algorithm is used to avoid complex calculations for the assumed top curve if all the calculated $m \times m$ points of the assumed top plane are far from the known top curve. Fourth, the assumed top curve of a PC track beam can be established by arranging the m points obtained in the previous step according to the criterion defined by the least square method. Finally, the criterion to assess the accuracy degree of the assumed top curve is established in the fractal dimension. This criterion postulates that the degree of coincidence between the supposed and the known top curves is high and that the accuracy of the curve that corresponds to the domain plane of the assumed bottom curve improves.

2. Deduction model of PC track beam curves

The deduction model of the PC track beam curve is shown in Fig. 4, where L_a is the assumed top curve, L_b is the known top curve, and L_c is the assumed bottom curve of a PC track beam, Point C is located in the known top curve L_b, point A is positioned in the assumed bottom curve L_c, and point B is deduced according to the geometric relationship shown in Fig. 5. The space curve L_a is composed of a series of assumed points B.

Fig. 1. Simply supported structure system

Fig. 2. Continuous structure system

Fig. 3. Monorail vehicle and track beams

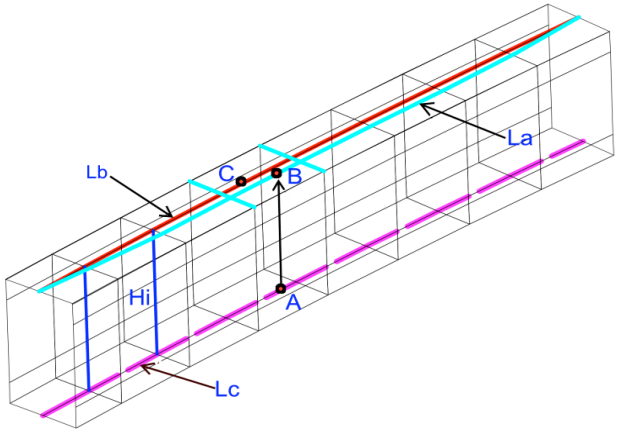

Fig. 4. Deduction model of the PC track beam curve

The geometric model of PC track beam deduction is depicted in Fig. 5 and explains the geometric relationship [8] of points A, B, and C. H_i is the height of a PC track beam and θ is the relation to parameters i_a, i_b, and i_v.

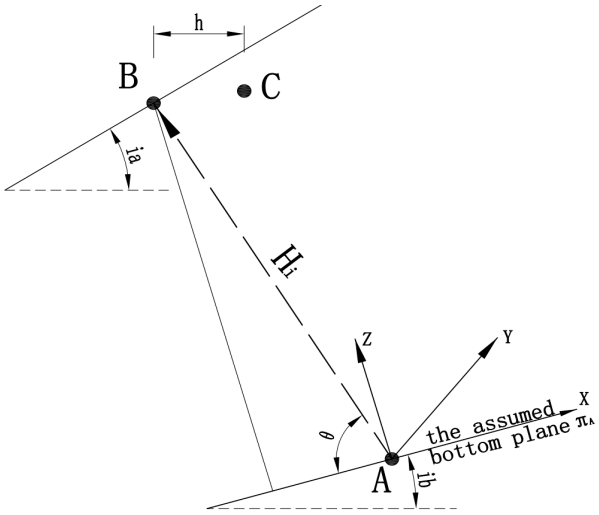

Fig. 5. Reversed geometric relationship for top curve deduction

$$\theta = f(i_a, i_b, i_v), \tag{1}$$

where i_a is the superelevation of the known top curve of a PC track beam; i_b is the dip angle between the bottom surface of

a PC track beam and the horizontal plane; and i_v is the longitudinal slope.

3. Establishment of the supposed top curve

The deduction model of a PC track beam curve has been elaborated in the previous section; however, the process of obtaining the supposed bottom curve L_a and supposed top curve remains unknown. Therefore, an elliptic plane π_A (Fig. 6) can easily be determined based on the PC track beam construction process. The point sets $\{A_{i,j}\}(i = 1, 2,\ldots, m, j = 1, 2,..., m)$ can be assumed by dividing plane π_A into m subsections. The corresponding supposed top curve domain plane π_B can also be obtained easily according to the geometric relationship presented in Fig. 5. The domain planes of the supposed top and bottom curves are exhibited in Fig. 6.

If an assumed top curve can be constructed by any point sets $P = \{P_i\}(i = 1,2,...,m)$ chosen from the division of domain plane π_B into $m \times m$ points and if only one point can be selected from one row at any time, then C_m^m supposed top curves can be determined. If all supposed top curves are compared with the known top curve L_b, then the computational quantity is large.

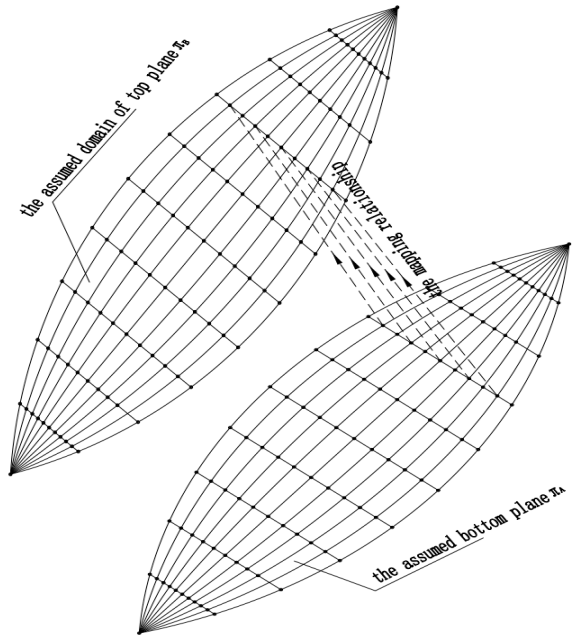

Fig.6. Mapping of two surfaces

3.1. Filtering of the point sets of the supposed top curve

Only one point is optimal in any row in the domain plane π_B; the other points are undesired. The dichotomy algorithm [9],[10] shown in Fig. 7 is used to filter the optimal point and to avoid large computational quantity.

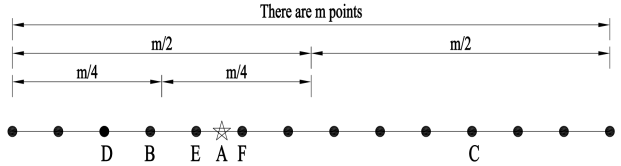

Fig.7. Diagram of minimum distance point selection

The mark "☆" represents a point that is in the known top curve, and "●" denotes the points that are in the supposed top curve domain π_B and in the k row.

Point A, which is marked as "☆," is one point in the known top curve L_b. The other points are marked as "●," such as B, C, D, E, and F. These points belong to domain plane π_B. Moreover, they are ordered in a row based on their distance in this domain plane. Points B and C are assumed to be the quarter points in the k row of plane π_B, and points D and E are the one-eighth points. The dichotomy algorithm is applied according to the following steps:

(1) The distances of points B and C to point A are represented by S_{AB} and S_{AC}. If the distance from point C to point A is greater than the distance from point B to point A, that is, $S_{AB} < S_{AC}$, then point B is better than point C. This outcome indicates that the other points on the right half of the row can be eliminated.

(2) The distances of one-eighth points D, E to point A are similarly computed and are denoted by S_{AD} and S_{AE}. If these distances are ordered as $S_{AE} < S_{AB} < S_{AD}$, then the other quarter points on the D side can be eliminated.

(3) As per a comparison of other distances with the method described in steps (1) and (2), F is the point nearest to A among those presented in Fig. 7, thus indicating that point F is the optimal point of the row selected from plane π_B.

(4) If all the optimal points of every row are selected to comprise the point sets $P = \{ P_i \}(i = 1, 2,..., m)$, then a supposed top curve L_a can be constructed with these sets. Fig. 8 shows a supposed top curve L_a that is fitted by points $P = \{ P_i \}(i = 1, 2,..., m)$.

3.2. Structural criterion of the supposed curve

Although the point sets $P = \{ P_i \}(i = 1, 2,..., m)$ of an assumed top curve are filtered by the dichotomy algorithm as described in section 3.1, the process of ordering these points and constructing an optimal supposed top PC track beam curve remains undeveloped. Therefore, a computer program is designed according to the least square method [11], [12], [13] and is elucidated as follows.

In the sets $\Phi = \mathrm{Span}\{\varphi_1, \varphi_2,\ldots, \varphi_n\}$, a known piece of data $(x_i, f_i)(i = 1, 2,\ldots, m)$ can be constructed as the following function.

$$S^*(x) = \sum a_k^* \varphi_k(x), (n < m) \tag{2}$$

The errors of this function are described as:

$$\delta_i = S^*(x_i) - f_i, (i = 1, 2,\ldots, m). \tag{3}$$

If the parameter $S^*(x)$ fits into the following equation:

$$\sum_{i=1}^{m} \omega(x_i)\delta_i^2 = \sum_{i=1}^{m} \omega(x_i)[S^*(x_i) - f_i]^2 = \min_{S(x)\in\phi} \sum_{i=1}^{m} \omega(x_i)[S^*(x_i) - f_i]^2 \tag{4}$$

where $\omega(x) \geq 0$ is the weight function defined in the range $[a, b]$, then the method presented above is the least square method and the parameter $S^*(x)$ that meets the requirement of Eq. (4) is the least squares solution that can be described by the following equation:

$$S^*(x) = a_0^* \varphi_0 + a_2^* \varphi_2 + \ldots a_n^* \varphi_n \tag{5}$$

To determine the solution to Eq. (5), the values of the following equation must be minimized as follows:

$$I(a_0,a_1,...,a_n)=\sum_{i=1}^{m}\omega(x_i)[\sum_{k=0}^{n}a_k\varphi_k(x_i)-f(x_i)]^2 \quad (6)$$

The minimal values of Eq. (6) are assumed to be $a_1^*,a_2^*,..,a_n^*$. With this minimization, Eq. (7) must be formulated:

$$\frac{\partial I}{\partial a_j}=0, \qquad (j=0,1, \ ..., \ n) \quad (7)$$

then

$$\sum_{i=1}^{m}\omega(xi)[\sum_{k=0}^{n}a_k\varphi_k(x_i)-f(x_i)]\varphi_j(x_i)=0 \quad (8)$$

The following parameters are assumed:

$$(\varphi_k,\varphi_j)=\sum_{i=1}^{m}\omega(x_i)\varphi_k(x_i)\varphi_j(x_i) \quad (9)$$

$$(f,\varphi_j)=\sum_{i=1}^{m}\omega(x_i)f(x_i)\varphi_j(x_i) \quad (10)$$

Then, the following equation can be obtained:

$$\sum_{k=0}^{n}(\varphi_k,\varphi_j)a_k=(f,\varphi_j), (j = 0, 1,..., n). \quad (11)$$

Given point set $\{x_i\}$ and weight function $\{\omega_i\}$ (i = 1, 2,…, m), if the coefficient functions $\varphi_0(x)$, $\varphi_2(x)$,…, $\varphi_n(x)$ meet the requirements of the following equation:

$$(\varphi_j,\varphi_k)=\sum_{i=1}^{m}\omega(x_i)\varphi_j(x_i)\varphi_k(x_i)=\begin{cases}0 & j\neq k\\ Ak>0 & j=k\end{cases} \quad (12)$$

Then the coefficient function $\{\omega_j\}_0^n$ is orthogonal and the coefficient matrix of Eq. (11) is simplified as a diagonal one.

$$a_k^*=\frac{(f,\varphi_k)}{(\varphi_k,\varphi_k)}=\frac{\sum_{i=1}^{m}\omega(x_i)f(x_i)\varphi_k(x_i)}{\sum_{i=1}^{m}\omega(x_i)\varphi_k^2(x_i)}, (k = 0, 1, 2,..., n) \quad (13)$$

If the primary data are assumed to be $(x_i, f_i)(i$ = 1, 2,…, m), then the least squares solution of the fitting curve can be described as follows:

$$S^*(x)=\sum_{k=0}^{n}\frac{(f,\varphi_k)}{(\varphi_k,\varphi_k)}\varphi_k(x), (k = 0, 1, 2,..., n) \quad (14)$$

4. Criterion for Accuracy Evaluation

If the supposed top curve L_a coincides completely with the known L_b, then the initial supposed curve L_c is the real solution for the bottom curve of a PC track beam. Unfortunately, the real bottom curve is difficult to measure; thus, a reasonable criterion must be established to assess the accuracy of a supposed bottom curve. The accuracy assessment criterion may be developed in the fractal dimension, and the error value is set to 0.005.

4.1. Box Fractal Dimension

The box dimension [14], [15], [16], [17] is a parameter to measure the fractal dimension. Assuming that F is a no-null subset of set Rn, $\delta(F)$ is the lowest subset count that can cover subset F. The maximum scale of $\delta(F)$ is defined as δ. The upper and lower box count dimensions $\overline{Dim}_BF$ and $\underline{Dim}_BF$ are defined as follows, respectively:

$$\overline{Dim}_BF=\overline{\lim_{\delta\to 0}}\frac{\log N_\delta(F)}{-\log\delta} \quad (15)$$

$$\underline{Dim}_BF=\underline{\lim_{\delta\to 0}}\frac{\log N_\delta(F)}{-\log\delta} \quad (16)$$

If $\overline{Dim}_BF$ is equal to $\underline{Dim}_BF$, then the aforementioned equations can be simplified as:

$$Dim_BF=\lim_{\delta\to 0}\frac{\log N_\delta(F)}{-\log\delta} \quad (17)$$

4.2. Initial estimation

Fig. 8 shows a spatial surface that is composed of the assumed top curve L_b and the known top curve L_a of a PC track beam. The initial assumed curve L_c can be identified as the real bottom curve of a PC track beam [18] if the considered parameters meet the following two requirements:

(1) The lengths of the curves S_a^L and S_b^L are almost similar; that is,

$$\frac{|S_a^L-S_b^L|}{S_a^L}\le 0.05 \quad (18)$$

where S_a^L and S_b^L represent the lengths of the curves L_a and L_b, respectively.

(2) The area of the space surface composed of curves L_a and L_b is approximately equal to zero or

$$A=\lim_{A_i\to 0}\sum_{i=1}^{N}A_i\approx 0 \quad (19)$$

where A_i is the area of each subsurface.

4.3. Optimization criterion

However, several defects may be detected in the aforementioned initial criterion because the degree of influence by certain factors is difficult to estimate accurately. These factors include curve superelevation as well as the span and height of a PC track beam. To overcome these complications, the fractal dimension is adopted to optimize the initial criterion. Fig. 8 illustrates the surface that is divided into a series of small sub-areas. Curves L_a and L_b are then divided into N sections [19], [20], and the length of each curve may be described as:

$$\delta_a^L=\frac{S_a^L}{N} \quad (20)$$

$$\delta_a^L=\frac{S_b^L}{N} \quad (21)$$

where δ_a^L and δ_b^L are the lengths of the sub-sections of curves L_a and L_b.

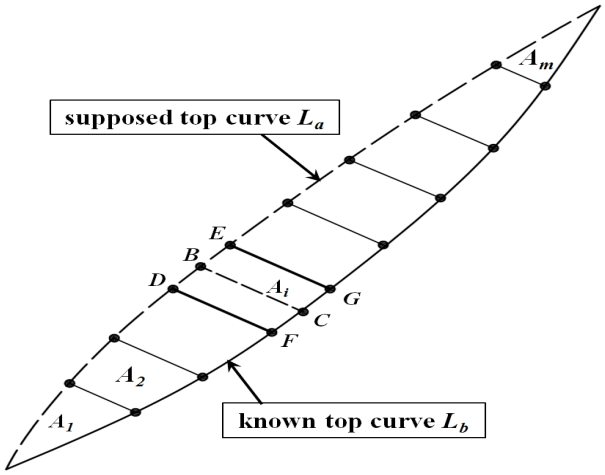

Fig.8. Surface composed of the assumed and known top curves

Assuming that curves L_a and L_b are divided M times [14], [15], the sub-sections are denoted by N_j (j = 1, 2,..., M) each time and the micro area scale of each sub-section is δ_j^A. To overcome the differences in parameter δ_j^A during each iteration, the main axis of each micro element replaces the sub-area. Fig. 9 displays a micro element DEGF of the surface presented in Fig. 9. δ_a^L is the length of sub-section DE, δ_b^L is the length of sub-section GF, h_1 is the length of EG, and h_2 is the length of DF. Points B and C represent the middle parts of sub-sections DE and GF, respectively. δ_H is the length of BC and is defined as the length of the major axis of the micro element DEGF. δ_H is calculated by Eq. (22).

$$\delta_H = \frac{h_1 + h_2}{2} \tag{22}$$

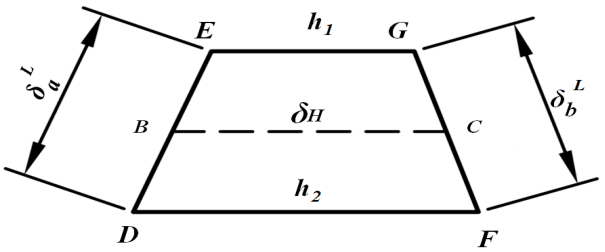

Fig. 9. Micro elements of a surface

The major axis δ_H may reach zero ($\delta_H \to 0$) as the area of A_i reaches zero ($A_i \to 0$) as well. Therefore, the supposed scale δ is set to a range of 2 mm to 5 mm in this study. Upon dividing the surface into N_j sub-areas (j = 1, 2,..., M), the number K_j of micro elements with a major axis that is longer than scale δ is determined. The box-counting fractal dimension [21], [22] D_s is defined as:

$$D_s = \lim_{N \to \infty} \sum_{j}^{M} \frac{K_j}{N_j} \tag{23}$$

Eq. (23) is equivalent to Eqs. (18) and (19); therefore, the accuracy assessment criterion of the assumed curve may be estimated with Eq. (23). In practical application, the initial assumed curve can be fully regarded as the real solution to the bottom curve of a PC track beam if the fractal dimension D_s computed with Eq. (23) is less than or equal to 0.05 (or $D_s \leq 0.05$).

5. Practical application

Given 10 pieces of PC track beams as an example, the fractal dimensions calculated with the aforementioned method are shown in the following table. The relation of the fractal dimension with division time is depicted in Fig. 10.The fractal dimension D_s is a dimensionless coefficient, and the unit of division degree is time.

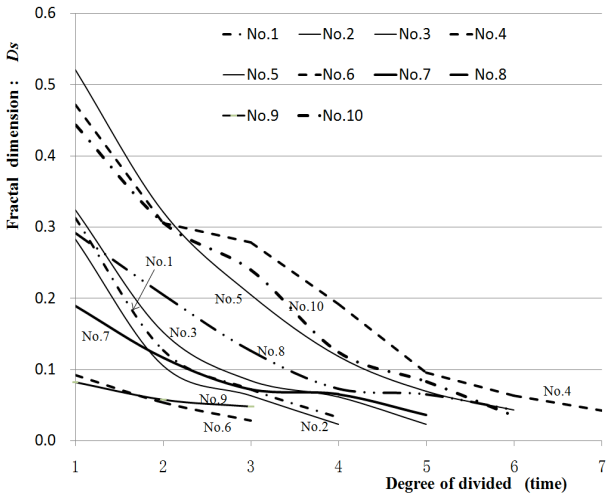

Fig.10. Fractal dimension vs. division time

Table 1. Fractal dimension (Ds) of each PC track beam

Times \ PC No.	01	02	03	04	05	06	07	08	09	10
1	0.312	0.283	0.324	0.472	0.521	0.092	0.189	0.291	0.082	0.443
2	0.127	0.105	0.152	0.305	0.321	0.053	0.116	0.205	0.057	0.306
3	0.072	0.063	0.084	0.278	0.205	0.028	0.072	0.126	0.048	0.239
4	0.032	0.023	0.061	0.192	0.118		0.065	0.073		0.124
5			0.023	0.095	0.069		0.036	0.065		0.083
6				0.063	0.043			0.043		0.035
7				0.042						

As per Fig. 10 and Tab. 1, the decrease in all the fractal dimension D_s values with increases in partition time and decrease speed is not uniform. The difference is mainly caused by influencing factors, such as the span and element of the known curve.

5.1. Factors affecting division time

(1) The number of divisions is proportional to the span of a PC track beam (for instance, the span of No. 08 is longer than that of No. 02).
(2) The number of divisions is inversely proportional to the radius of the known top curve (for instance, the radius of No. 03 is smaller than that of No. 04).
(3) The number of divisions is proportional to the superelevation of the known top curve (for instance, the superelevation of No. 04 is greater than that of No. 10).
(4) The number of divisions is proportional to the superelevation rate of the known top curve (for instance, the superelevation rate of No. 10 is greater than that of No. 01).

5.2. Factors affecting the decay rate of fractal dimensions

(1) The span of a PC track beam extends with a slow decay rate (No. 08).
(2) The curve radius of a PC track beam shrinks with a slow decay rate (No. 10).
(3) The superelevation of a PC track beam curve is enhanced with a slow decay rate (No. 05).
(4) The superelevation rate of a PC track beam increases with a slow decay rate (No. 05).
(5) The decay rate of the fractal dimension of a linear PC track beam is accelerated to its maximum, the circular PC track is slow, and the transition curve of the PC track beam decelerates to its minimum.

6. Conclusions

A reverse model that is dissimilar from conventional methods is established to identify the parameters of PC track beam curves. If the domain of the bottom curve of a PC track beam is assumed to be a spindle plane, then this model contrarily deduces the corresponding spindle domain of the assumed top curves. The assumed top curve derived from a domain of such curves is optimized. If the degree of coincidence between this constructed curve and the known top curve meets certain requirements, then the corresponding bottom curve can be considered the real bottom curve of a PC track beam. This technique is confirmed to be valid and feasible, and the main conclusions drawn from this study are presented below:
(1) The deduction model of PC track beam curve parameters is established in a manner contrary to conventional methods. The known top curve is regarded as a standard to assess the accuracy of the assumed top curve, and the deduction model determined according to the reversed approach sufficiently ensures the accuracy of the theoretical derivation and of the calculation results.
(2) The surface comprising the assumed and known top curves is regarded as the research object. Instead of comparing the shapes of these two curves directly, the coincidence degree between both curves is assessed by calculating the area of this surface. This process transfers the known top curve from the Euclidean geometry space to the fractal dimension space, thereby creating the basis of the assessment criterion established in the fractal dimension.
(3) The assumed top curve is constructed with the dichotomy algorithm and the least square method; this curve is compared with the known top curve based on the fractal dimension to avoid unnecessary calculations and to ensure the accuracy of the goal curve.
(4) The length δ_h of the major axis of the subsurface is regarded as the assessment threshold to facilitate selection among different mesh scales and to ensure the consistency of evaluation standards each time. The influence of various mesh scales is reflected completely on the other two minor axes; therefore, the assessment threshold of the major axis can be a constant value.
(5) The discrete algorithms, theoretical assumptions, and deduction method presented in this paper are easily realized with computer programs. Thus, this study lays a foundation for their application in practical engineering.

Acknowledgements

The authors acknowledge the financial support provided by the Science and Technology Project of the Chongqing Administration of Land, Resources and Housing (No.CQGT-KJ-2012021) and the Program for Changjiang Scholars and Innovative Research Team in University (No. IRT1045).

References

1. Han J., "The design evaluation of PSC track beam in Korean straddle monorail transit and software development for controlling the PSC track beam manufacture". *In Beijing, Beijing Jiaotong University*, 2011.
2. Zhou Y., "Design and research of monorail transportation". *Southwest Jiaotong University*, 2002.
3. Siu L. K., "Innovative lightweight transit technologies for sustainable transportation". *Journal of Transportation Systems Engineering and Information Technology*, 7(2), 2007, pp. 63-71.
4. Li X. M., Li Z. G., "Study on the construction technology of inverted T shaped PC track beam of Chongqing monorail". *Architectural Engineering*, 15(6), 2010, pp. 33-36
5. Zhong M. L., Zhu E. Y., "Development of emergency track beam alignment for rapid track beam replacement of straddle monorail transit". *Journal of Transportation Engineering*, 13(9), 2013, pp. 416-423.
6. Xu G., Zhu E.Y., Xu R. L., "Study on the construction method of PC track beam". *Research & Application of Building Materials*, 18(1), 2004, pp. 24-26.
7. Zhu Y. L., Meng Q. F., "Fabrication techniques of straddle-type monorail PC track girders". *Urban Mass Transit*, 9(8), 2006, pp. 47-52.
8. Yao Y. B., "A simple and convenient arithmetic for the transformation of plane co-ordinate system". *Journal of Geomatics*, 1, 2001, pp. 1-3.
9. Alexander W., "Dichotomy for finite tournaments of mixed-type". Discrete Mathematics, 33(8), 2015, pp. 2523–2538
10. Larry G., Nets H. K., "On the erodes distinct distances problem in the plane". *Annals of Mathematics*, 1(9), 2010, pp. 155-190.
11. Ding K. L, Sheng Y. Z, Ou J. K., "Methods of line-fitting based on total least-squares". *Journal of Liaoning Technical University*, 29(1), 2010, pp. 44-47.
12. Guo S. Y., Zhai W. J., Tang Q., "Combining the Hough transform and an improved least squares method for line detection". *Computer Science*, 39(4), 2012, pp. 196-200.
13. Qi B. Q., "Logging curve fitting with centralized least square method". *Well Logging Technology*, 31(4), 2007, pp. 331-334.
14. Zheng X, Lin G. X., Wang J. Z., "Image analysis based measurement and calculation of fractal characteristic of pore structure of peanut cake". *2010 Second International Conference on Modeling, Simulation and Visualization Methods*, 2010, pp. 83-86.
15. Zhang T. F., Wu Y. Q., "Research on two fractal box dimension". *Journal of Jilin Jianzhu University,* 30(4), 2013, pp. 84-84.

16. Zachary G., Mathew T., "Simulation of fractional Brownian surfaces via spectral synthesis on manifolds", *IEEE Transactions on Image Processing,* 23(10), 2014, pp. 4383-4388.
17. Mae T., Asayama S., "Architectural design and structure of computer-generated arch with fractal geometric form". *American Society of Civil Engineers*, 23(9), 2014, pp. 748-755.
18. Zhao X. B., "Application of wavelets to rock components classification". *Journal of Information & Computational Science*, 11(17), 2014, pp. 6229-6244.
19. Martino G. D., Iodice A., Riccio D., and Ruello G., "Imaging of fractal profiles", *IEEE Transactions on Geoscience and Remote Sensing*, 48(8), 2010, pp. 3280-3289.
20. Chicharro F., Cordero A., Torregrosa J. R., "Dynamics and fractal dimension of steffensen-type methods", *Algorithms*, 8(2), 2015, pp. 271-279.
21. Xiang G. S., Jiang H., Xu Y. F., "Surface fractal dimension of bentonite from nitrogen adsorption". *Soil Behavior and Geomechanics ASCE*, 34(4), 2014, pp. 286-292.
22. Song J. H., Kim C., "3-D topology optimization based on nodal density of divided sub-elements for enhanced surface representation". *International Journal of Precision Engineering and Manufacturing*, 13(4), 2012, pp. 557-563.